Proc. Natl. Acad. Sci. USA
Vol. 86, pp. 9228–9232, December 1989
Biochemistry

Aspartic acid-96 is the internal proton donor in the reprotonation of the Schiff base of bacteriorhodopsin

(site-specific mutagenesis/proton pump/purple membrane/photocycle/photovoltage)

HARALD OTTO*, THOMAS MARTI†, MARTIN HOLZ*, TATSUSHI MOGI†‡, MANFRED LINDAU*, H. GOBIND KHORANA†, AND MAARTEN P. HEYN*

*Biophysics Group, Freie Universität Berlin, Arnimallee 14, D-1000 Berlin 33, Federal Republic of Germany; and †Departments of Biology and Chemistry, Massachusetts Institute of Technology, 77 Massachusetts Avenue, Cambridge, MA 02139

Contributed by H. Gobind Khorana, September 12, 1989

ABSTRACT **Above pH 8 the decay of the photocycle intermediate M of bacteriorhodopsin splits into two components: the usual millisecond pH-independent component and an additional slower component with a rate constant proportional to the molar concentration of H^+, $[H^+]$. In parallel, the charge translocation signal associated with the reprotonation of the Schiff base develops a similar slow component. These observations are explained by a two-step reprotonation mechanism. An internal donor first reprotonates the Schiff base in the decay of M to N and is then reprotonated from the cytoplasm in the N → O transition. The decay rate of N is proportional to $[H^+]$. By postulating a back reaction from N to M, the M decay splits up into two components, with the slower one having the same pH dependence as the decay of N. Photocycle, photovoltage, and pH-indicator experiments with mutants in which aspartic acid-96 is replaced by asparagine or alanine, which we call D96N and D96A, suggest that Asp-96 is the internal proton donor involved in the re-uptake pathway. In both mutants the stoichiometry of proton pumping is the same as in wild type. However, the M decay is monophasic, with the logarithm of the decay time [log (τ)] linearly dependent on pH, suggesting that the internal donor is absent and that the Schiff base is directly reprotonated from the cytoplasm. Like H^+, azide increases the M decay rate in D96N. The rate constant is proportional to the azide concentration and can become >100 times greater than in wild type. Thus, azide functions as a mobile proton donor directly reprotonating the Schiff base in a bimolecular reaction. Both the proton and azide effects, which are absent in wild type, indicate that the internal donor is removed and that the reprotonation pathway is different from wild type in these mutants.**

Bacteriorhodopsin (bR) is a light-driven proton pump from *Halobacterium halobium* that transports H^+ ions from the cytoplasm to the extracellular space with a stoichiometry of one proton per cycle (1). The transmembrane H^+ translocation involves distinct electrogenic steps associated with H^+ ejection from the protein interior into the periplasm and the subsequent H^+ rebinding from the cytoplasmic side of the membrane. The proton uptake occurs on the millisecond time scale and is apparently coupled to the reprotonation of the Schiff base (SB) and the decay of the M intermediate of the photochemical cycle. Fourier transform infrared (FTIR) spectroscopy first indicated that several aspartate carboxyl groups undergo protonation changes during the photocycle (2, 3). Site-directed mutagenesis of bR showed that substitution of aspartate residues at positions 85, 96, and 212 by asparagine reduced the proton pumping activity to a few percent (4) and revealed, in combination with FTIR measurements, the protonation states of specific aspartate residues in various photocycle intermediates (5, 6). In the mutant D96N, the kinetics of proton uptake is affected (7–9). We recently showed that the low steady-state proton pumping activity of D96N (3% of wild-type at pH 7) is due to a kinetic defect: the pump is turning over ≈30 times slower than in wild type with the same stoichiometry. This is due to a corresponding slowdown in the decay of M and the associated charge movement (9). The logarithm of the reprotonation time constant in D96N is proportional to the pH, suggesting that the SB is reprotonated directly from the cytoplasm in this mutant (9). We proposed that Asp-96 serves as an internal proton donor in the reprotonation of the SB and presented a minimal two-step scheme for the proton uptake process (9). We now present direct evidence for the existence of two steps from the pH dependencies of both the M decay and the slow electrical charge translocation in wild type. We propose a kinetic model for the proton-uptake phase involving an N-to-M back reaction and an internal donor. We confirm and extend the identification of Asp-96 as this internal proton donor, using the new mutant D96A.

MATERIALS AND METHODS

Preparation of bR Mutants. The construction of the gene coding for the mutant D96N, its expression in *Escherichia coli*, the purification of the bacterioopsin apoprotein, and the regeneration with retinal in 1% DMPC/CHAPS {L-α-dimyristoyl phosphatidylcholine/3-[(3-cholamidopropyl)dimethylammonio]-1-propanesulfonate} micelles have all been described (4). The preparation of the additional mutant D96A was by identical procedures. The mutant apoproteins were also regenerated and reconstituted in vesicles with the polar lipids from *H. halobium* in a 1:1 weight ratio (HL-vesicles) (10).

Photocycle Measurements. The photocycle was measured with a home-made flash-photolysis spectrometer. The samples were excited with flashes (5 ns) from a 30-mJ excimer laser (EMG 50, Lambda Physik), which pumped a broadband dye laser [rhodamine 6G (590 nm) or coumarin 153 (510 nm)] at a repetition rate of $<0.1\ s^{-1}$. Data were acquired with a personal computer (Compaq Deskpro 386/20e) equipped with a 40-MHz two-channel A/D converter with eight-bit resolution and 128-kbyte memory (T12840, Geitmann GmbH, 5750 Menden, FRG). In each of the two channels, 65536 data

The publication costs of this article were defrayed in part by page charge payment. This article must therefore be hereby marked "*advertisement*" in accordance with 18 U.S.C. §1734 solely to indicate this fact.

Abbreviations: bR, bacteriorhodopsin; DMPC, L-α-dimyristoyl phosphatidylcholine; CHAPS, 3-[(3-cholamidopropyl)dimethylammonio]-1-propanesulfonate; HL-vesicles, bR or its mutants reconstituted in vesicles consisting of the polar lipids of *Halobacterium halobium* in a 1:1 weight ratio; D96N and D96A, bR mutants in which aspartic acid-96 has been replaced by asparagine or alanine, respectively; SB, unprotonated Schiff base.

‡Present address: Department of Biology, University of Tokyo, Bunkyo-ku, Tokyo, Japan.

points were simultaneously sampled (0.1 and 100 μs per point, respectively) after filtering with corresponding time constants. The linearly spaced data points were reduced to 1024 logarithmically spaced time points by appropriate averaging. Absorbance data were collected at 17 wavelengths varying in steps of 20 nm from 350 to 670 nm, and a global fit at all wavelengths was obtained with one set of exponentials. Alternatively, the data at a single wavelength were fitted with a sum of up to seven exponentials.

Time-Resolved Photovoltage Measurements. Photovoltage was measured on bR HL-vesicles adsorbed to black lipid membranes as described (9, 11).

Kinetics of Proton Release and Uptake. The pH changes associated with proton release and uptake were measured at pH 7.3 by using the indicator dye pyranine (8-hydroxyl-1,3,6-pyrenetrisulfonate; pK 7.2) as described (9).

RESULTS

Photocycle and Charge Translocation of bR at Alkaline pH. The photocycle of bR changes considerably between pH 6 and pH 10. Whereas at pH 6 the O intermediate is observed with little evidence for the N intermediate, at pH 10 N accumulates and O appears to be absent (12, 13). An extremely slow component develops in the decay of the M intermediate with increasing pH contributing ≈20–40% of the signal (Fig. 1 *Inset*). The additional slow component becomes detectable near pH 8. Fig. 1 shows that the fast decay time is only weakly dependent on pH, whereas the slow component has linear dependence of log (τ) on pH with a slope of ≈1. This suggests that during the slow decay of M, a group within the protein is being protonated directly from the bulk aqueous phase. For such a reaction, one expects as a first approximation a rate constant k proportional to $[H^+]$ and thus a log (τ) plot showing linear dependence on pH with a slope of 1.0. Associated with the decay of M and the reprotonation of the SB is a millisecond component in the photovoltage signal corresponding to charge translocation from the cytoplasm to the SB (11). To determine if the slow

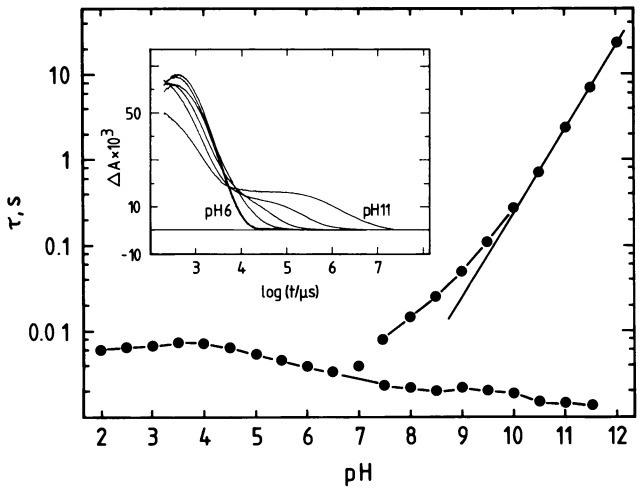

FIG. 1. The fast and slow decay times τ of the photocycle intermediate M of bR in purple membranes are plotted logarithmically as a function of pH. The slope of the straight line is 1.0. (*Inset*) Time course of the corresponding absorbance changes at 410 nm from pH 6 to pH 11 in steps of 1. The decay curves at pH 6 and pH 7 are nearly identical. Conditions were: 150 mM KCl, 30 mM sodium phosphate buffer, dark-adapted, 22°C, and excitation at 590 nm with 3 mJ per flash. The fast and slow phases are not well described by single exponentials. Thus, the decay times given here are lumped values of neighboring time constants exhibiting a parallel pH dependence and similar amplitude spectra in multi-wavelength experiments.

photocycle component is accompanied by a charge movement, the influence of pH on the photovoltage kinetics was measured. In Fig. 2 *Inset*, typical electrical signals are presented at pH 7.1 and pH 9.4. At pH 9.4 an additional slow 0.8-s component is observed (arrows), which is absent at pH 7.1. In Fig. 2, the log of the time constants of the two slowest electrical components is plotted as a function of pH. A bifurcation is observed similar to that of Fig. 1, with a pH-independent component in the 10-ms range and a slower component with log (τ) linearly dependent on pH. The data provide direct evidence that the proton transfer from the cytoplasm to the SB occurs in at least two sequential steps, one being strongly pH dependent and probably associated with the reprotonation of a group within the protein.

Two-Step Model for the Reprotonation of the SB and Proton Uptake from the Cytoplasm. The data of Figs. 1 and 2 may be explained by the simple two-step model shown in Fig. 3 for the photocycle intermediates and proton movements involved in the decay of M and the reprotonation of the SB. The spectroscopic states and the associated H^+ movements are shown in Fig. 3 *Upper* and *Lower*, respectively. The model involves an internal proton donor that is assumed to be protonated in the ground state at any pH. The SB is reprotonated by the internal donor (rate constant k_1), and at low pH the donor is reprotonated immediately from the cytoplasm ($k_2[H^+] >> k_1$). Thus, k_1 is rate-limiting, and only a single component is observed electrically when protons are abundant. In the M state, the SB is deprotonated and the donor is protonated. Since at alkaline pH the decay of N is slowed down with k proportional to $[H^+]$ (13, 14), we assume that reprotonation of the donor is coupled to the decay of N. Thus, we attribute the spectroscopic state N to a protein state in which the SB is reprotonated, but the internal donor is still deprotonated. At low pH N will decay very rapidly once it is formed ($k_2[H^+] >> k_1$), and it will not accumulate. We propose that the decay of N is coupled to the decay of M through a back reaction (k_{-1}). With k_{-1} smaller than k_1, the back reaction can be neglected at low pH, and both the decay of M and the associated charge movement will have only one decay time determined by k_1. With pH > log (k_2/k_1), the reprotonation of the donor and the decay of N become rate limiting ($k_2[H^+] < k_1$), and N accumulates. Two components

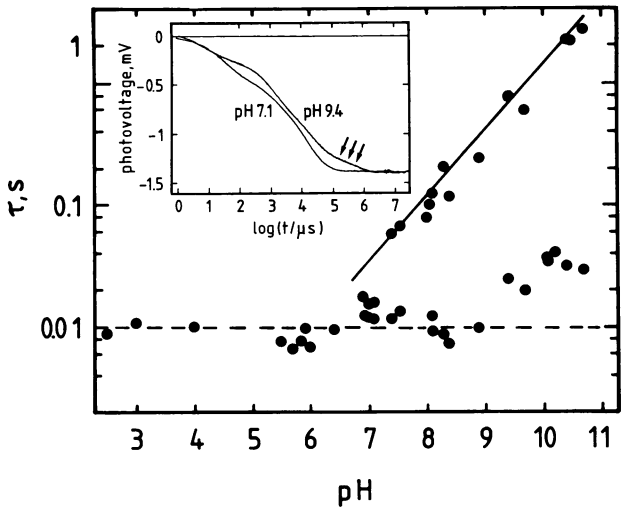

FIG. 2. The time constants of the two slowest photovoltage components in purple membranes plotted logarithmically against pH. The slope of the straight line is 0.55. (*Inset*) Time course of the charge displacement in bR at pH 7.1 and pH 9.4. Arrows indicate the additional slow component at pH 9.4. The system discharge ($\tau \approx 2$s) has been removed by deconvolution (9). Purple membranes were adsorbed to a 6-μm-thick Teflon support; conditions otherwise were as in Fig. 1.

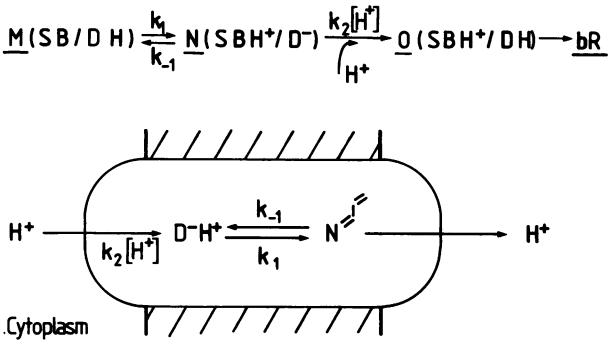

FIG. 3. Two-step kinetic model for the reprotonation of the unprotonated SB from the cytoplasm. (*Upper*) Spectroscopic states M, N, O, and bR with corresponding protonation states of the SB and the donor (D). (*Lower*) Proton movements corresponding to the transitions between M, N, O, and bR (SB and D drawn in M state).

are now predicted in the H^+ translocation and decay of M: the first one pH independent with time constant $\tau = 1/(k_1 + k_{-1})$, and the second slower one pH dependent with $\tau = 1/k_2[H^+]$. Because of the quasi-stationary N–M equilibrium, the pH-dependent slow decay of N will show up as the slow component of M. The source of the slow pH-dependent component of M is thus the pH-dependent rate constant for the N decay. The ratio of the amplitudes of the slow and fast components of the decay of M at high pH is given by k_{-1}/k_1. Inspection of the *Inset* of Fig. 1 shows that this ratio is between 0.4 and 0.2. The differential equations associated with the kinetic model of Fig. 3 were solved both analytically and numerically. Two decay times are predicted for the decay of M. With $k_1 = 300\ s^{-1}$, $k_{-1} = 80\ s^{-1}$, and $k_2 = 4 \times 10^{10}\ M^{-1}\cdot s^{-1}$, the calculated decay times (τ_1 and τ_2) and corresponding amplitudes (A_1 and A_2) are in reasonable agreement with the data (Fig. 4). With these rate constants, the critical pH at which the bifurcation occurs is $\log(k_2/k_1) = 8.1$. Below this pH, A_2 is close to zero and only the millisecond component (τ_1) is observed. At alkaline pH, the two components coexist with detectable amplitudes, and the dependence of $\log(\tau_1)$ on pH is linear, whereas τ_2 is essentially pH independent. Our analysis shows that the proton uptake occurs in two steps at any pH. However, only at alkaline pH can they be separately observed.

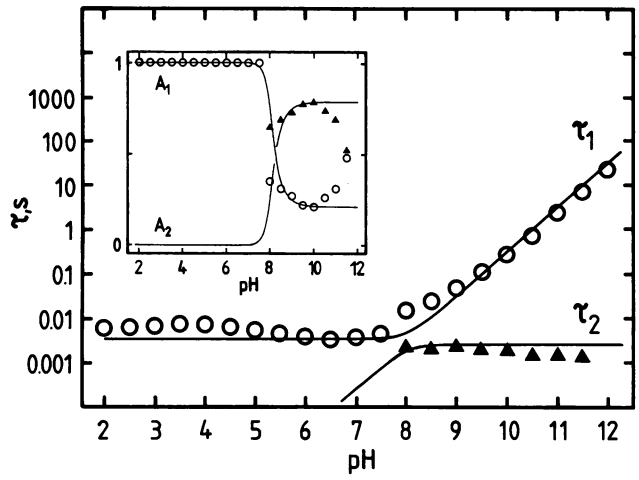

FIG. 4. Comparison of experimental data and predictions of kinetic model for the time constants τ_1 and τ_2 and corresponding amplitudes A_1 and A_2 (*Inset*) of the M decay of purple membranes as a function of pH. The solid curves were calculated with $k_1 = 300\ s^{-1}$, $k_{-1} = 80\ s^{-1}$, and $k_2 = 4 \times 10^{10}\ M^{-1}\cdot s^{-1}$. Above pH 8, τ_1 and τ_2 are the slow and fast decay times, respectively. Below pH 8 only τ_1 is observed since the amplitude A_2 vanishes.

Photocycle and Charge Displacement for D96N and D96A. The mutants D96N (4) and D96A regenerate the wild-type chromophore with absorption maxima of 552 and 553 nm, respectively, and show a normal bathochromic shift upon light adaptation. For both mutants, the extent of chromophore formation is comparable to wild type (≈85%), although the rates are slightly decreased. Thus, it is clear that these mutants are in all respects, except for proton-pumping, quite similar to wild type and most likely folded in the same way. This is also supported by x-ray diffraction experiments for D96N (9). The proton pumping activity of D96A and D96N at pH 7 is only 2% and 3%, respectively, of ebR (bacteriorhodopsin prepared by expression of a synthetic wild-type gene in *E. coli*). In both mutants the decay of M is very much slowed down at neutral pH and is strongly pH dependent. The pH dependence of the M decay time constants for D96A and D96N are shown in Fig. 5. The decay of M in D96A is somewhat slower than in D96N. For both mutants, $\log(\tau)$ is proportional to pH with a slope of ≈0.8 over a wide pH range except at low pH where the mutants start to turn blue. It should be noted that, in contrast to wild type, the decay of M has only one component in both mutants at every pH. Taken together these results show that Asp-96 functions as the internal proton donor: in the mutants, having no internal donor, the SB is reprotonated directly from the cytoplasm in a bimolecular reaction leading to the extreme pH dependency. Accordingly, the data of Fig. 5 show that at low pH the decay of M is accelerated to millisecond values, and the effect of the mutation can apparently be overcome by adding enough protons. The photovoltage measurements with D96A show that the proton movement associated with the decay of M is likewise monophasic and slowed down with respect to wild type in the same pH-dependent manner (Fig. 5). The results are in good agreement with those previously obtained for D96N (9).

In contrast to the kinetics, the stoichiometry of H^+ release and uptake is unaffected by the mutation. This is shown for D96A in Fig. 6, where the kinetics of the proton exchange as sensed by the dye pyranine is compared with the rise and decay of M. From the signal amplitude, the stoichiometry was calculated to be ≈0.9 protons per bR cycling, which is similar to the values previously obtained for wild type and the

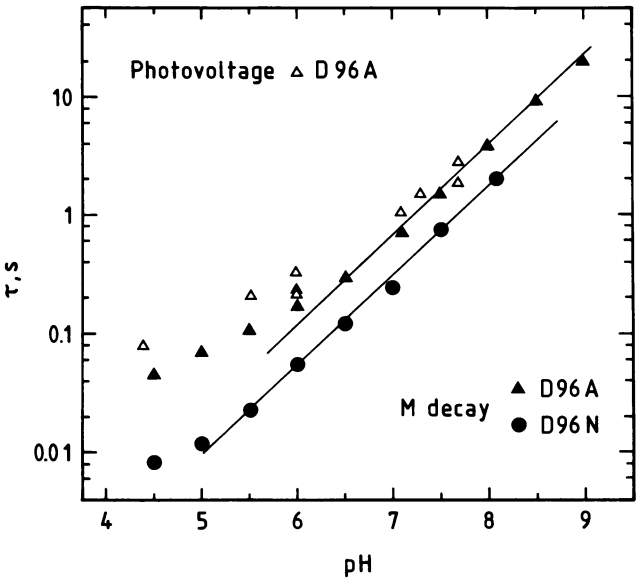

FIG. 5. The time constants of the M decay in HL-vesicle preparations of D96A and D96N and of the slow photovoltage component of D96A plotted logarithmically as a function of pH. The slope of the straight lines is 0.75. Conditions were as in Figs. 1 and 2.

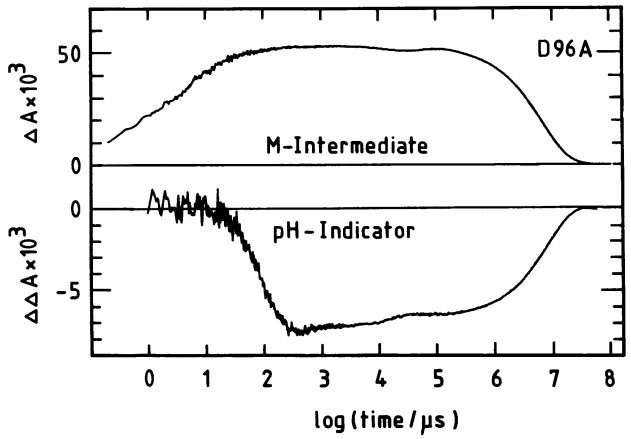

FIG. 6. Traces: upper, rise and decay of the M intermediate of D96A in DMPC/CHAPS micelles at pH 7.3 as monitored by the absorbance change at 410 nm; lower, absorbance change of pyranine at 450 nm for the same sample, reflecting the release and uptake of protons by D96A. Conditions were: 150 mM KCl, 22°C, excitation wavelength of 590 nm, repetition rate of 0.015 s^{-1}, 4 mJ, and dark-adapted. The exponential time constants for the M decay and the proton uptake are 7.3 and 7.5 s, respectively.

D96N mutant (9). The proton uptake occurs with the same time constant as the decay of M.

Effect of Azide on the Photocycle and Charge Translocation of D96N and D96A. Azide is known to accelerate the decay of the M intermediate in halorhodopsin (15). Similar observations have been reported for the mutant D96N of bR (16). Fig. 7*A* shows the time course of the M intermediate of D96N at pH 6 for various azide concentrations. The most obvious feature of Fig. 7*A* is the marked acceleration of the M decay with increasing azide concentrations. The decrease in amplitude of the 410-nm signal is at least partly due to the resulting overlap of the rise and decay phases. This concentration-dependent effect of azide is reminiscent of the effect of increasing $[H^+]$ (see Fig. 5). Accordingly, in Fig. 7*B* log (τ) is plotted versus log $[NaN_3]$ at pH 6 and pH 7.5. At pH 7.5 the slope is −1 over a wide concentration range (from 0.5 to 1024 mM), corresponding to the slope of +1 in the log (τ) versus pH plot. In contrast, azide has only minor effects on wild-type. Interestingly, azide cannot only overcome the kinetic defect of the mutation at constant pH, but also can make the decay of M 2 orders of magnitude faster than in the wild type. At very high azide concentrations, some deviation from linearity is observed, which could be taken as evidence for saturation. However, when the pH was lowered from 6 to 5.5 (Fig. 7*A*, second lowest trace) and 5.0 (lowest trace) at 512 mM azide, the decay time of M became as fast as 74 μs, which is ≈100 times faster than in wild type. Thus, there is no indication of saturation for the accelerating effect of azide and pH on the M decay. At pH 7.5 the O intermediate is not observed in the photocycle of D96N (9). However, accelerating the M decay by adding 80 mM azide or by doing the experiment at pH 5 in the absence of azide (9) results in a rather normal photocycle including the O intermediate, suggesting that the absence of O is due to the changed kinetics of the M → O transition. The similarity between the effects of protons and azide, in particular the slopes of about −1 in the log (τ) versus log [concentration] plots, suggest that the protonated form of azide enters the protein interior and acts as a mobile proton donor. Since azide has a pK of ≈4.8, $[HN_3]$ is much higher at pH 6 than at pH 7.5. Thus, the rate at pH 6 should be faster by ≈1.47 log units (Fig. 7*B*, dashed line), which is rather close to the observed shift. This pH effect and the slope of −1 provide strong evidence that the SB

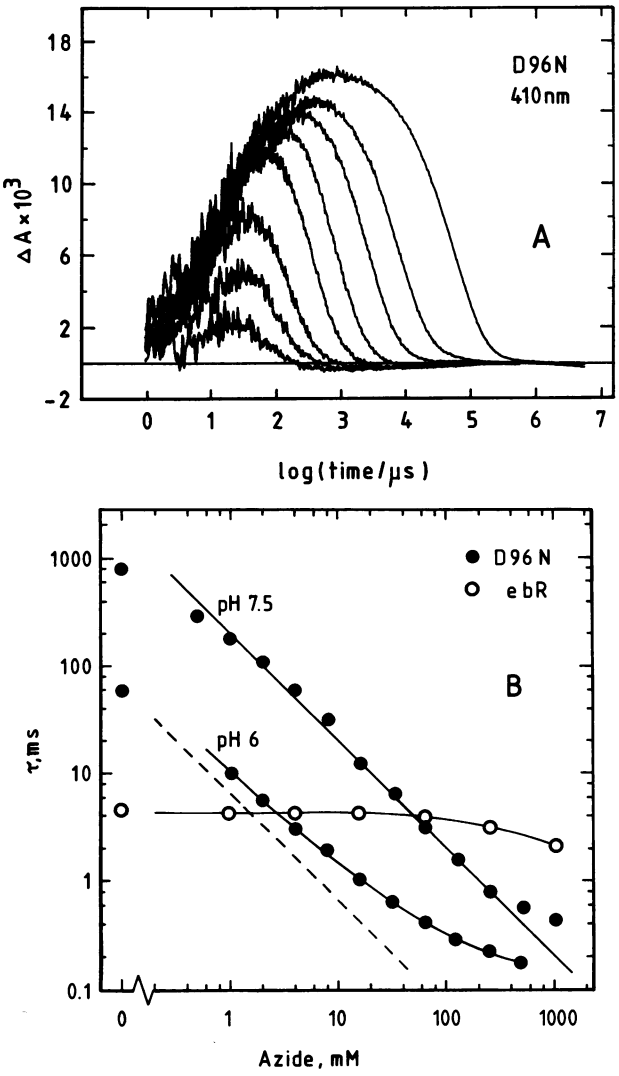

FIG. 7. (*A*) Rise and decay of the M intermediate of the mutant D96N (absorbance change at 410 nm) at various azide concentrations. From right to left, the first six traces are at pH 6.0 and $[NaN_3]$ = 0, 1, 4, 16, 64, and 512 mM. The last two traces are at 512 mM NaN_3 and pH 5.5 and pH 5.0. (*B*) Double-logarithmic plot of the decay time of M versus $[NaN_3]$ for D96N at pH 7.5 and pH 6.0 and for wild type at pH 7.5. The straight lines have a slope of −1. HL-vesicles were used; otherwise conditions were as in Fig. 1.

is reprotonated by the protonated azide HN_3 in a bimolecular reaction.

The decay of M remains essentially monophasic in the presence of azide. There is a gradual shift of the time constant and not a new fast azide-induced component. This behavior strongly suggests that azide exerts its effect on D96N and D96A by a dynamic association–dissociation equilibrium that is faster than the observed M decay.

Unpublished experiments on D96A also show that azide speeds up the slow charge translocation in a similar way (see also ref. 16). The charge movements in the presence of azide occur in the same direction as in its absence, indicating that azide acts from the cytoplasmic side of the membrane.

DISCUSSION

In the photocycle of bR, at low pH, an O intermediate can be observed with little evidence for N, whereas at high pH the amplitude of O becomes very small and N dominates (12, 13). The rate constant for the N → O transition is apparently

strongly pH dependent so that at low and neutral pH the decay of N is faster than its rise, whereas at high pH the decay of O is faster than its rise. It was recently observed (13, 14) that the decay rate constant of N increases linearly with the free $[H^+]$ and that the slow M component has a parallel pH dependence. No significance was attached to these dependencies on the external $[H^+]$, and the slow M was instead ascribed to a different species in the photocycle (slow and fast M; ref. 13). A back reaction from O to M has been considered in previous investigations of the photocycle (17), but the intermediate O is not observed at alkaline pH. The introduction of an N → M back reaction (see also ref. 18) solves the problems of different M decay times: there is only one M, but since M is coupled to N by a back reaction, the slow pH-dependent decay time of N shows up in the decay of M. The observed pH-dependent N decay (13) leads to the same pH dependency for the slow component of the M decay (Fig. 1). Recent kinetic resonance Raman data also show that N and the slow component of M decay together (19). The slow and fast components of M also have exactly the same resonance Raman spectrum (20), consistent with the idea of a single homogeneous M. We interpret the pH dependence of the N decay and the corresponding splitting of M decay and charge translocation at alkaline pH in fast and slow components as due to the reprotonation of an internal proton donor from the cytoplasm. Whereas the existence of a proton donor group inside the protein has been postulated in the past (13, 21), the electrical data at high pH provide the first direct evidence for charge motion associated with the reprotonation of the donor. Thus, the reprotonation of the SB occurs in at least two steps, each associated with the movement of charge. We introduced a minimal model to explain the main features of our data. We also analyzed more complicated models. By allowing the donor to deprotonate in the ground state at very high pH for instance, we can explain the deviation between the experimental amplitudes and the model prediction in this pH region (Fig. 4 *Inset*).

In the mutants D96N (9) and D96A, the decay of M is monophasic and strongly pH dependent throughout, suggesting that the internal donor is absent. Asp-96 appears to be in a hydrophobic environment and remains protonated in the ground state at least up to pH 9 (3). Fourier transform infrared measurements indicate that in the photocycle Asp-96 remains protonated until the decay of M (6), consistent with its postulated deprotonation in the M → N transition. The SB is located in the middle of the membrane (22), and Asp-96 is located approximately halfway between the SB and the cytoplasmic end of helix C (R. Henderson, personal communication). Thus, Asp-96 is in a proper position to serve as an internal donor in the proton-uptake pathway. In the electrical measurements at pH 9.4, the ratio of the amplitudes of the 800-ms component associated with the reprotonation of the donor and the 20-ms component corresponding to the H^+ transfer from the donor to the SB was $\approx 3/8$. The electrical amplitudes are thus in reasonable agreement with the proposed position of Asp-96 in the structure. As noted, the slope of the plots of log (τ) versus the surface pH is expected to be one. Measured and plotted is the dependence on the bulk pH, however. That the slope in these plots is occasionally somewhat less than 1 may be explained by the fact that the surface pH is smaller than the bulk pH and that the difference is largest at high pH. In all respects the mutant D96A has properties similar to D96N.

It was of interest to test D96A, since the side chain of asparagine may still be able to form a hydrogen bond. Like D96N, D96A is a mutant with minimal perturbation in the absorption spectrum, light–dark adaptation, and regeneration kinetics. The M decay of D96A is slightly slower than that of D96N (see Fig. 5) in accordance with the lower steady-state proton pumping activity. The data presented on D96A confirm our previous conclusion (9) that the defect in these mutants is due to the slow turnover of the pump. The fact that in both mutants the M decay rate constant increases in proportion to $[H^+]$ or $[HN_3]$, which is not observed in wild type, shows that the internal donor is removed. They differ from wild type in terms of the accessibility of the SB for protons and azide during the photocycle. The way in which protons are funneled to the SB leading to its protonation appears to be changed.

We thank J. Tittor for bringing the azide effect to our attention prior to publication. This work was supported by grants from the National Institutes of Health (R01 GM28289-09 and AI11479) and the Office of Naval Research (N00014-82-K-0668) to H.G.K. and a grant from the Deutsche Forschungsgemeinschaft (Sfb 312, TPB1) to M.P.H.; T. Marti is the recipient of a fellowship from the Swiss National Science Foundation.

1. Khorana, H. G. (1988) *J. Biol. Chem.* **263,** 7439–7442.
2. Rothschild, K. J., Zagaeski, M. & Cantore, W. A. (1981) *Biochem. Biophys. Res. Commun.* **103,** 483–489.
3. Engelhard, M., Gerwert, K., Hess, B., Kreutz, W. & Siebert, F. (1985) *Biochemistry* **24,** 400–407.
4. Mogi, T., Stern, L. J., Marti, T., Chao, B. H. & Khorana, H. G. (1988) *Proc. Natl. Acad. Sci. USA* **85,** 4148–4152.
5. Braiman, M. S., Mogi, T., Marti, T., Stern, L. J., Khorana, H. G. & Rothschild, K. J. (1988) *Biochemistry* **27,** 8516–8520.
6. Gerwert, K., Hess, B., Soppa, J. & Oesterhelt, D. (1989) *Proc. Natl. Acad. Sci. USA* **86,** 4943–4947.
7. Marinetti, T., Subramaniam, S., Mogi, T., Marti, T. & Khorana, H. G. (1989) *Proc. Natl. Acad. Sci. USA* **86,** 529–533.
8. Butt, H. J., Fendler, K., Bamberg, E., Tittor, J. & Oesterhelt, D. (1989) *EMBO. J.* **8,** 1657–1663.
9. Holz, M., Drachev, L. A., Mogi, T., Otto, H., Kaulen, A. D., Heyn, M. P., Skulachev, V. P. & Khorana, H. G. (1989) *Proc. Natl. Acad. Sci. USA* **86,** 2167–2171.
10. Popot, J.-L., Gerchman, S.-E. & Engelman, D. M. (1987) *J. Mol. Biol.* **198,** 655–676.
11. Holz, M., Lindau, M. & Heyn, M. P. (1988) *Biophys. J.* **53,** 623–633.
12. Scherrer, P. & Stoeckenius, W. (1985) *Biochemistry* **24,** 7733–7740.
13. Kouyama, T., Nasuda-Kouyama, A., Ikegami, A., Mathew, M. K. & Stoeckenius, W. (1988) *Biochemistry* **27,** 5855–5863.
14. Kouyama, T. & Nasuda-Kouyama, A. (1989) *Biochemistry* **28,** 5963–5970.
15. Hegemann, P., Oesterhelt, D. & Steiner, M. (1985) *EMBO J.* **4,** 2347–2350.
16. Tittor, J., Soell, C., Oesterhelt, D., Butt, H. J. & Bamberg, E. (1989) *EMBO J.* **8,** 3477–3482.
17. Parodi, L. A., Lozier, R. H., Bhattacharjee, S. M. & Nagle, J. F. (1984) *Photochem. Photobiol.* **40,** 502–512.
18. Ames, J. B., Fodor, S. P. A. & Mathies, R. A. (1989) *Biophys. J.* **55,** 254 (abstr.).
19. Fodor, S. P. A., Ames, J. B., Gebhard, R., van den Berg, E. M. M., Stoeckenius, W., Lugtenburg, J. & Mathies, R. A. (1988) *Biochemistry* **27,** 7097–7101.
20. Ames, J. B., Fodor, S. P. A., Gebhard, R., Raap, J., van den Berg, E. M. M., Lugtenburg, J. & Mathies, R. A. (1989) *Biochemistry* **28,** 3681–3687.
21. Drachev, L. A., Kaulen, A. D., Skulachev, V. P. & Zorina, V. V. (1987) *FEBS Lett.* **226,** 139–144.
22. Hauss, T., Otto, H., Grzesiek, S., Westerhausen, J. & Heyn, M. P. (1989) *Biophys. J.* **55,** 254 (abstr.).